Crystal Structures of Thermoelectric *n*- and *p*-type Ba₈Ga₁₆Ge₃₀ Studied by Single Crystal, Multitemperature, Neutron Diffraction, Conventional X-ray Diffraction and Resonant Synchrotron X-ray Diffraction

Mogens Christensen, Nina Lock, Jacob Overgaard, and Bo B. Iversen*

*Contribution from the Department of Chemistry, University of Aarhus,
DK-8000 Aarhus C, Denmark*

Received June 6, 2006; E-mail: bo@chem.au.dk

Abstract: Comprehensive single-crystal structural investigations of *n*- and *p*-type $Ba_8Ga_{16}Ge_{30}$ have been carried out using multitemperature neutron and conventional X-ray diffraction as well as resonant synchrotron X-ray diffraction. The data show that the guest atom positions and dynamics are very similar in the two structures, although the barium atoms are slightly more displaced from the cage centers in the *p*-type structure than in the *n*-type structure ($\Delta d = 0.025$ Å). For both structures Fourier difference maps calculated from very high-resolution neutron diffraction data ($\sin \theta/\lambda > 2$ Å^{-1}) show that the Ba nuclear density at lowest temperatures (15 K) is distributed in a torus around the crystallographic *6d* site with maxima in the *24j* positions. At room temperature the maxima have shifted to the *24k* position. Analysis of atomic displacement parameters give Einstein temperatures of ~60(1) K for both structures. Thus, the fundamental difference in the low temperature thermal conductivity observed for *p*- and *n*-type $Ba_8Ga_{16}Ge_{30}$ appear not to be directly related to the guest atom behavior as is commonly assumed in thermoelectric research. The neutron data and the resonant synchrotron X-ray data facilitate refinement of Ga/Ge framework occupancies. The Ga atoms have a clear preference for the *6c* site with the preference being somewhat stronger for the *n*-type structure.

Introduction

Thermoelectric research has seen a strong revitalization since the "phonon glass electron crystal" (PGEC) concept was introduced by Slack in 1995.[1] Qualitatively speaking the ideal thermoelectric material should conduct heat like a glass but electrons like a crystal. This will lead to a high thermoelectric figure of merit (ZT), $ZT = TS^2\sigma/\kappa$, where S is the thermopower, σ is the electrical conductivity, and κ is the thermal conductivity. Based on the PGEC concept semiconducting host–guest materials such as skutterudites and clathrates have been targeted in hundreds of studies, and many seminal contributions have appeared.[2]

The crux of the PGEC materials is the very low lattice thermal conductivities (κ_L), which have been intensely discussed since the discovery of the glasslike magnitude and temperature dependence of κ_L in *n*-type $Sr_8Ga_{16}Ge_{30}$ and *n*-type

$Eu_8Ga_{16}Ge_{30}$.[3] Initially, it was proposed that guest atom tunneling in combination with resonant phonon scattering were responsible for the glasslike κ_L in some of the highly crystalline clathrates.[4] This appeared to be corroborated by the absence of a glasslike κ_L in *n*-type $Ba_8Ga_{16}Ge_{30}$, where neutron diffraction experiments showed that the cation nuclear density distribution is more localized than those in $Sr_8Ga_{16}Ge_{30}$ and $Eu_8Ga_{16}Ge_{30}$.[4b] However, later a glasslike κ_L was also observed in *p*-type $Ba_8Ga_{16}Ge_{30}$.[5] Different models have been proposed for explaining the glasslike dip in κ_L including disorder scattering related to the displacement of the guest atoms,[6] four-well tunneling,[7] and a soft potential model for the guest atoms.[8] To account for the fundamental difference in κ_L between *n*- and *p*-type $Ba_8Ga_{16}Ge_{30}$ all these models implicitly assume that the crystal structures of *n*- and *p*-type $Ba_8Ga_{16}Ge_{30}$ are significantly different. Recently Bentien et al. proposed that the κ_L behavior

(1) Slack, G. A. *New Materials and Performance Limits for Thermoelectric Cooling*; Rowe, D. M., Ed.; CRC Press: Boca Raton, FL, 1995.
(2) (a) Sales, B. C.; Mandrus, D.; Williams, R. K. *Science* **1996**, *272*, 1325–1328. (b) Keppens, V.; Mandrus, D.; Sales, B. C.; Chakoumakos, B. C.; Dai, P.; Coldea, R.; Maple, M. B.; Gajewski, D. A.; Freeman, E. J.; Bennington, S. *Nature* **1998**, *395*, 876–878. (c) Tritt, T. M. *Science* **1999**, *283*, 804–805. (d) DiSalvo, F. J. *Science* **1999**, *285*, 703–706. (e) Chung, D.; Hogan, T.; Brazis, P.; Rocci-Lane, M.; Kannewurf, C.; Bastea, M.; Uher, C.; Kanatzidis, M. G. *Science* **2000**, *287*, 1024–1027. (f) Venkatasubramanian, R.; Siivola, E.; Colpitts, T.; O'Quinn, B. *Nature* **2001**, *413*, 597–602. (g) Hsu, K. F.; Loo, S.; Guo, F.; Chen, W.; Dyck, J. S.; Uher, C.; Hogan, T.; Polychroniadis, E. K.; Kanatzidis, M. G. *Science* **2004**, *303*, 818–821. (h) Snyder, G. J.; Christensen, M.; Nishibori, E.; Caillat, T.; Iversen, B. B. *Nat. Mater.* **2004**, *3*, 458–463.
(3) (a) Nolas, G. S.; Cohn, J. L.; Slack, G. A.; Schujman, S. B. *Appl. Phys. Lett.* **1998**, *73*, 178–180. (b) Cohn, J. L.; Nolas, G. S.; Fessatidis, V.; Metcalf, T. H.; Slack, G. A. *Phys. Rev. Lett.* **1999**, *82*, 779–782.
(4) (a) Nolas, G. S.; Weakley, T. J. R.; Cohn, J. L.; Sharma, R. *Phys. Rev. B* **2000**, *61*, 3845–3850. (b) Sales, B. C.; Chakoumakos, B. C.; Jin, R.; Thompson, J. R.; Mandrus, D. *Phys. Rev. B* **2001**, *63*, 245113. (c) Paschen, S.; Carrillo-Cabrera, W.; Bentien, A.; Tran, V. H.; Baenitz, M.; Grin, Y.; Steglich, F. *Phys. Rev. B* **2001**, *64*, 214404.
(5) Bentien, A.; Christensen, M.; Bryan, J. D.; Sanchez, A.; Paschen, S.; Steglich, F.; Stucky, G. D.; Iversen, B. B. *Phys. Rev. B* **2004**, *69*, 045107.
(6) Bridges, F.; Downward, L. *Phys. Rev. B* **2004**, *70*, 140201.
(7) Zerec, I.; Keppens, V.; McGuire, M. A.; Mandrus, D.; Sales, B. C.; Thalmeier, P. *Phys. Rev. Lett.* **2004**, *92*, 185502–18550.4.
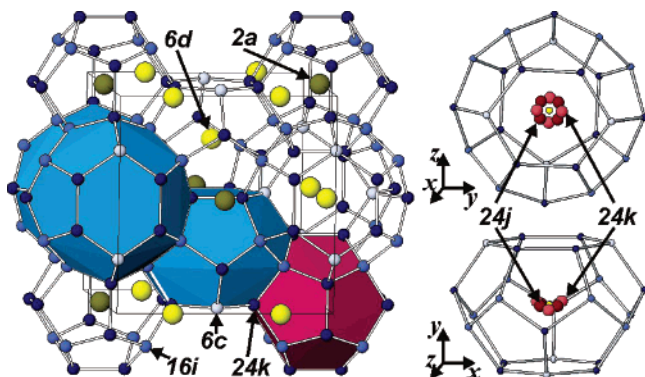(8) Umeo, K.; Avila, M. A.; Sakata, T.; Suekuni, K.; Takabatake, T. *J. Phys. Soc. Jpn.* **2005**, *74*, 2145–2148.

Figure 1. Type I clathrate structure. The host structure sites are *6c* (light), *16i* (medium) and *24k* (dark). The M(2) atoms are light, whereas M(1) atoms are dark.

of clathrates is determined by strong phonon charge carrier scattering.[9] This is a somewhat controversial conclusion, which differs fundamentally from the models focusing on the guest atoms. Analysis based on all available transport data established a strong correlation between κ_L and the charge carrier properties. The model of Bentien et al. does not require a large structural difference between *n*- and *p*-type $Ba_8Ga_{16}Ge_{30}$. Guest atom tunneling in clathrates was recently documented for Eu_8Ga_{16}-Ge_{30},[10] but this tunneling may not significantly influence the behavior of κ_L in the temperature range where the dip is observed.[11]

In general the structure of a material is the foundation on which microscopic physical theories are formulated to explain material properties. The interconnection between the crystal structures of *n*- and *p*-type $Ba_8Ga_{16}Ge_{30}$ and current theories on an essential thermoelectric property (κ_L) provides a good example of structure−property relations. In order to understand the thermoelectric properties of clathrates it is necessary that comprehensive structural analysis is done on both *n*- and *p*-type $Ba_8Ga_{16}Ge_{30}$. Type I clathrates typically have cubic structures belonging to space group $Pm\bar{3}n$, although different symmetries have been observed in defect structures.[12] The unit cell of the host framework consists of two dodecahedral and six larger tetrakaidecahedral cages; see Figure 1. The cages are formed by three distinct crystallographic sites with Wyckoff notation *6c*, *16i*, and *24k*. Cations are encapsulated inside the cages, and if centered in the small cage they are on the *2a* site (denoted M1), whereas the center of the large cage is the *6d* site (denoted M2). The clathrates with Ga/Ge host structures have received particular attention due to their optimization potential for thermoelectric applications.[13] The unit cell content can generally be written as $M_8Ga_{16-x}Ge_{30+x}$, where M = Eu, Sr, and Ba. The charge carrier type is controlled through variation of *x*, where $x > 0$ gives *n*-type properties and $x < 0$ gives *p*-type properties.[5]

Most attention has focused on the guest atoms and their specific positions in the two different cages. As explained above many theories on the glasslike κ_L in clathrates implicitly assume that the positions and thermal behavior of Ba atoms in *n*- and *p*-type $Ba_8Ga_{16}Ge_{30}$ are significantly different. However, the host structure also plays an important role for the thermoelectric properties, e.g., through disorder and vacancy scattering. It is difficult to determine the exact host structure due to the very similar scattering powers of Ga and Ge for both X-rays and neutrons. For neutrons the scattering lengths are $b(Ga) = 0.73$ fm and $b(Ge) = 0.81$ fm, whereas for X-rays the contrast is even worse with Ga having 31 electrons and Ge having 32 electrons. In many crystallographic studies of Ga/Ge clathrates the 16 Ga atoms are assumed to be randomly distributed over the 46 framework sites.[14] However, early on maximum entropy method (MEM) analysis of X-ray diffraction data on $Sr_8Ga_{16}Ge_{30}$ and $Ba_8Ga_{16}Ge_{30}$ actually found a preference for Ga at the *6c* site and that Ga avoids the *16i* site.[15] This result was later supported by the framework siting observed in other clathrates where the scattering contrast is much larger.[16] More recently resonant powder diffraction measurements on *n*-type Sr_8Ga_{16}-Ge_{30} have also supported the result of the MEM analysis,[17] but so far no reliable quantitative assessments have been given for the host structure ordering. As an example the refined occupancies from the $Sr_8Ga_{16}Ge_{30}$ resonant powder diffraction data sum to give a strongly *p*-type material for a crystal that is *n*-type.[17] In order to shed more light on the difference between the *p*- and *n*-type $Ba_8Ga_{16}Ge_{30}$ and thereby substantiate or disprove the theories on the glasslike κ_L, we have investigated two samples using single-crystal neutron, conventional X-ray, and resonant synchrotron X-ray diffraction. In the following we denote *n*-type $Ba_8Ga_{16}Ge_{30}$ as n-Ba and *p*-type $Ba_8Ga_{16}Ge_{30}$ as p-Ba.

Experimental Section

Synthesis. The single crystal of n-Ba was prepared by the Czokralski method by pulling it from a melt of conventionally synthesized $Ba_8Ga_{16}Ge_{30}$. The melt was prepared from stoichiometric amounts of Ga/Ge/Ba, which were placed in a corundum crucible. The crucible was sealed in a steel bomb under Ar, placed in a vertical furnace, and heated above the melting temperature of Ge followed by cooling to room temperature. For the synthesis of p-Ba a flux method was used.[15] 75 wt % of Ga was added to n-Ba powder followed by heat treatment. Nice facetted crystals were isolated from the Ga matrix and washed with concentrated HCl. The sign of the charge carriers was determined by measurement of the thermopower, which is positive for p-Ba and negative for n-Ba.

Multitemperature Neutron Diffraction. Single-crystal neutron diffraction data were measured during two separate beam time periods on the SCD instrument at the Intense Pulsed Neutron Source (IPNS), Argonne National Laboratory.[18] The n-Ba single crystal was cut from the Czokralski pulled rod to approximate dimensions of $2 \times 2 \times 2$

(9) Bentien, A.; Johnsen, S.; Iversen, B. B. *Phys. Rev. B* **2006**, *73*, 094301.

(10) Hermann, R. P.; Keppens, V.; Bonville, P.; Nolas, G. S.; Grandjean, F.; Long, G. J.; Christen, H. M.; Chakoumakos, B. C.; Sales, B. C.; Mandrus, D. *Phys. Rev. Lett.* **2006**, *97*, 017401.

(11) Umeo, K.; Avila, M. A.; Sakata, T.; Suekuni, K.; Takabatake, T. *J. Phys. Soc. Jpn.* **2005**, *74*, 2145−2148.

(12) (a) Dubois, F.; Fassler, T. F. *J. Am. Chem. Soc.* **2005**, *127*, 3264−3265. (b) Carrillo-Cabrera, W.; Budnyk, S.; Prots, Y.; Grin, Y. *Z. Anorg. Allg. Chem.* **2004**, *630*, 2267−2276. (c) Carrillo-Cabrera, W.; Gil, R. C.; Paschen, S.; Grin, Y. *Z. Kristallogr.* **2002**, *217*, 183−185.

(13) (a) Bentien, A.; Pacheco, V.; Paschen, S.; Grin, Y.; Steglich, F. *Phys. Rev. B* **2005**, *71*, 165206. (b) Saramat, A.; Svensson, G.; Palmqvist, A. E. C.; Stiewe, C.; Mueller, E.; Platzek, D.; Williams, S. G. K.; Rowe, D. M.; Bryan, J. D.; Stucky, G. D. *J. Appl. Phys.* **2006**, *99*, 023708.

(14) (a) Chakoumakos, B. C.; Sales, B. C.; Mandrus, D. G.; Nolas, G. S. *J. Alloys Compd.* **2000**, *296*, 80−86. (b) Chakoumakos, B. C.; Sales, B. C.; Mandrus, D. G. *J. Alloys Compd.* **2001**, *322*, 127−134.

(15) Bentien, A.; Palmqvist, A. E. C.; Bryan, J. D.; Latturner, S.; Stucky, G. D.; Furenlid, L. ; Iversen, B. B. *Angew. Chem., Int. Ed.* **2000**, *39*, 3613−3616.

(16) (a) Bentien, A.; Nishibori, E.; Paschen, S.; Iversen, B. B. *Phys. Rev. B* **2005**, *71*, 144107. (b) Bentien, A.; Iversen, B. B.; Bryan, J. D.; Stucky, G. D.; Palmqvist, A. E. C.; Schultz, A. J.; Henning, R. W. *J. Appl. Phys.* **2002**, *91*, 5694−5699.

(17) Zhang, Y. G.; Lee, P. L.; Nolas, G. S.; Wilkinson, A. P. *Appl. Phys. Lett.* **2002**, *80*, 2931−2933.

(18) Schultz, A. J. *Trans. Am. Cryst. Assoc.* **1993**, *29*, 29−41.

Table 1. Details for the Refinement of Four Different Models for Ba(2) against the 100 K Neutron Diffraction Data[a]

neutron	n-Ba model				p-Ba model			
	Ba1 2a (x,y,z) = (0,0,0) U_{iso} = 56(4) 6c (x,y,z) = (¹/₄, 0, ¹/₂), host U_{iso} = 65(4) 16i (x,x,x) = 0.184 53(4) 24k (x,y,z) = (0, 0.308 43(6), 0.118 04(6)) a = 10.758(1) Å				Ba1 2a (x,y,z) = (0,0,0) U_{iso} = 51(2) 6c (x,y,z) = (¹/₄, 0, ¹/₂), host U_{iso} = 53(1) 16i (x,x,x) = 0.184 56(2) 24k (x,y,z) = (0, 0.308 56(3), 0.118 03(3)) a = 10.760(2) Å			
model name	N-JI	N-JA	N-KI	N-KA	N-JI	N-JA	N-KI	N-KA
Ba(2) position	24j	24j	24k	24k	24j	24j	24k	24k
ADP description	iso	aniso	iso	aniso	Iso	aniso	iso	aniso
x	0.25(-)	0.25(-)	0.2475(14)	0.2439(24)	0.25(-)	0.25(-)	0.2498(6)	0.2433(9)
y	0.4893(5)	0.4925(47)	0.5(-)	0.5(-)	0.4876(2)	0.4883(4)	0.5(-)	0.5(-)
z	0.9893(5)	0.9925(47)	0.0153(6)	0.0117(45)	0.9876(2)	0.9883(4)	0.0172(2)	0.0131(6)
distance to 6d (Å)	0.163(7)	0.115(72)	0.167(7)	0.142(44)	0.188(2)	0.178(6)	0.185(3)	0.158(7)
U_{11}	114(4)	114(9)	114(9)	114(9)	90(2)	90(2)	90(4)	90(4)
U_{22}	114(4)	199(90)	114(9)	140(48)	90(2)	130(13)	90(4)	279(34)
U_{33}	114(4)	199(90)	114(9)	240(110)	90(2)	130(13)	90(4)	107(20)
U_{12}		−24(26)				−2(4)		
U_{13}		24(26)		46(38)		2(4)		13(10)
U_{23}		−8(76)				1(9)		
N_{par}	19	22	20	23	19	22	20	23
N_{obs}	10 284	10 284	10 284	10 284	15 127	15 127	15 127	15 127
$(N_{obs}(I_{obs} > 3\sigma(I_{obs})))$	(2971)	(2971)	(2971)	(2971)	(6779)	(6779)	(6779)	(6779)
R_{F}	48.6	48.6	48.5	48.5	29.2	29.2	29.2	29.2
$(R_{F}(I_{obs} > 3\sigma(I_{obs})))$	(18.6)	(18.6)	(18.6)	(18.6)	(12.5)	(12.5)	(12.5)	(12.5)
R_{wF}	22.8	22.8	22.8	22.8	16.7	16.7	16.7	16.7
$(R_{wF}(I_{obs} > 3\sigma(I_{obs})))$	(12.6)	(12.6)	(12.6)	(12.6)	(12.2)	(12.2)	(12.2)	(12.2)
R_{wI}	31.1	31	31	31	24.6	24.5	24.6	24.5
$(R_{wI}(I_{obs} > 3\sigma(I_{obs})))$	(19.8)	(19.8)	(19.8)	(19.8)	(19.2)	(19.2)	(19.3)	(19.2)

[a] The resolution of the data is 2.16 Å^{-1} for p-Ba and 2.08 Å^{-1} for n-Ba. The ADPs have been multiplied by 10^4 Å^2. See text for explanation of different models.

mm^3, and diffraction data were measured at 25, 100, 200, and 295 K. The p-Ba crystal was isolated from the Ga matrix and shaped into a sphere of radius 1.7 mm. Data were measured at 15, 50, 100, 200, 300, 500, and 700 K. Temperature control below room temperature was obtained with a closed cycle Displex helium refrigerator. For the elevated temperatures the p-Ba crystal was placed in a quartz tube, which was wrapped in a platinum foil resistance heater. It is noteworthy that for all data sets the resolution in reciprocal space is extremely high (sin $\theta/\lambda > 2$ Å^{-1}). Thus, the number of unique reflections is 5−10 times larger than in most single-crystal diffraction studies reported in the literature. The extreme data resolution allows the study of subtle disorder features. The high data resolution is a great advantage of the white beam time-of-flight method compared to monochromatic studies. Since the flux grown p-Ba crystal is larger than the Czokralsky pulled n-Ba crystal, the diffraction intensities are stronger for p-Ba, and consequently the p-Ba data sets contain more significant reflections. The perfection of the p-Ba crystal also leads to more extinction in the low order data, where 58 reflections have y < 0.7 for p-Ba at 300 K compared with only 6 reflections for n-Ba. Excluding the highly extinct reflections from the refinements has no significant influence on the agreement factors, the occupancy refinement, or the nuclear density of the barium guest atoms. At elevated temperatures the number of significant reflections is much reduced due to the drastically increasing Debye−Waller factor. To address the issue of extinction and reproducibility of the subtle nuclear density features, a smaller crystal of p-Ba (0.9 mm radius) was studied at room temperature (referred to as p-Bas). For this crystal 43 reflections had y < 0.7. Further information is given in the Supporting Information.

The neutron scattering intensities were integrated and corrected for absorption effects with the program ANVRED.[19] Since equivalent reflections are measured at different wavelengths the data are not averaged. This leads to higher residual factors than those normally observed in monochromatic studies, but as shown by Overgaard et al.

the refined structural parameters from TOF data are highly accurate.[20] The data were used for structural refinements with the program GSAS.[21] There are two central issues to be addressed: (i) the description of Ba(2) and (ii) the Ga/Ge framework siting. When this information is extracted from the diffraction data by least-squares modeling, there will inevitably be problems with parameter correlation. For Ba(2) the positional parameters correlate with the ADPs, while for the framework it is especially the occupancies that correlate with the ADPs. The correlations can be handled by introducing various constraints in the refinements, and below a large number of different models are described that in different ways attempt to counter the fundamental parameter correlation problem.

Initial refinements were carried out with a model, referred to as 1-N, where Ba(2) was centered on the 6d site, and the framework was fully disordered such that each site of the three host structure crystallographic sites is occupied by 34.78% Ga and 65.22% Ge. Subsequently framework occupancies were allowed to refine, but convergence was not achieved in free refinements. In model 2-N two constraints were imposed: (1) a chemical constraint fixing the amount of Ga and Ge to 16 and 30 atoms per unit cell, respectively, and (2) a full occupancy constraint on all framework sites. The Ba(2) guest atoms can occupy two different sites around the 6d site, namely the 24j and 24k sites; see Figure 1. The Ba(2) siting was tested against four models using the 100 K data with framework occupancies fixed to the results of the 2-N model. Thus models with Ba(2) at the 24j site with isotropic (N-JI) and anisotropic ADPs (N-JA) were refined as well as models with Ba(2) at the 24k site with isotropic (N-KI) and anisotropic ADPs (N-KA). Details of the refinements are listed in Table 1. The description of Ba(2) from the N-JI model was used in refinements of the multitemperature data (model 3-N) since there are negligible differences in reliability factors between N-JI and N-KI (Table 1), and N-JI has fewer free parameters. The detailed results of refinements with models 1-N, 2-N, and 3-N are given in the Supporting Information. The

(19) (a) Schultz, A. J.; Leung, P. C. W. *J. Phys. (Paris) Colloq. C* **1986**, *5*, 137−142. (b) Schultz, A. J. *Trans. Am. Crystallogr. Assoc.* **1987**, *23*, 61−69.

(20) Overgaard, J.; Schiøtt, B.; Larsen, F. K.; Iversen, B. B. *Chem.−Eur. J.* **2001**, 3756−3767.
(21) Larson, A. C.; Dreele, R. B. V. *Los Alamos National Laboratory Report LAUR* 2004; pp 86−748.

Table 2. Framework Occupancies Obtained from the Neutron and Resonant Synchrotron Data[a]

	6c % Ga	16i % Ga	24k % Ga	6c % Ge	16i % Ge	24k % Ge	6c % total	16i % total	24k % total	Ga	Ge	total
p-Ba neutron	60(4)	33(2)	30(2)	40(4)	67(2)	70(2)	100(6)	100(3)	100(2)	16(1)	30(1)	46(1)
p-Ba 4-X	64(1)	17(1)	39(1)	36(1)	83(1)	61(1)	100(2)	100(1)	100(1)	16.0(3)	30.0(3)	46.0(6)
p-Ba 7-X	63(5)	22(3)	37(3)	35(3)	77(2)	60(2)	98(8)	99(5)	96(4)	16.1(1.4)	28.7(9)	45(2)
n-Ba neutron	74(7)	17(2)	37(1)	26(7)	83(2)	63(1)	100(10)	100(2)	100(2)	16(1)	30(1)	46(1)
n-Ba 4-X	76(1)	16(1)	37(1)	24(1)	84(1)	63(1)	100(2)	100(1)	100(1)	16.0(3)	30.0(3)	46.0(6)
n-Ba 7-X	72(4)	17(3)	36(2)	25(2)	81(2)	61(1)	96(7)	98(4)	97(3)	15.6(1.2)	29.1(7)	45(2)

[a] For the neutron data model 2-N was used, and for the synchrotron data models 4-X and 7-X were used. See text for explanation of different models.

reliability factors for the different models do not differ significantly, and therefore they cannot be used to distinguish between the models.

Resonant Synchrotron X-ray Diffraction. Single-crystal synchrotron resonant X-ray diffraction data were measured at the Swiss-Norwegian beamlines at ESRF, France, during two separate beam time allocations. For n-Ba a small chip with dimensions of $30 \times 20 \times 6$ μm^3 was used, which originated from the crystal utilized in the neutron diffraction experiment. Data sets were collected using a six-circle Kuma diffractometer equipped with an Oxford CCD detector. Resonant diffraction data was measured at 100 K with an energy 2 eV below the absorption edge of Ga, which was found at 10.368 keV. For p-Ba a small crystal with a radius of ~6 μm was picked from the sand paper used to shape the neutron crystal. Resonant diffraction data was measured 3 eV below the Ga edge at 100 K. For all measurements the temperature was controlled with an Oxford nitrogen cryo-stream device.

The absorption edge of Ga was established by measuring the fluorescence signal as a function of the incoming wavelength. Anomalous scattering factors were calculated using the program CHOOCH.[22] For p-Ba the values were $f'(Ga) = -7.9$, $f''(Ga) = 0.7$, $f'(Ge) = -2.3$, $f''(Ge) = 0.6$, whereas for n-Ba the values were $f'(Ga) = -8.1$, $f''(Ga) = 0.8$, $f'(Ge) = -2.3$, $f''(Ge) = 0.6$. Therefore the scattering power difference between Ga and Ge amounts to about 7 electrons 2−3 eV below the Ga edge. Structure factors were extracted using the program CrysAlis.[23] For n-Ba, a face indexed absorption correction was carried out using the CrysAlis software, while program SORTAV was used for data averaging.[24] For p-Ba SORTAV was used for both empirical absorption correction and data averaging. Structural refinements were carried out with neutral atom form factors using SHELX.[25]

A total of eight models were tested against the data using different constraints. In all models Ba(2) was held at the center of the cage at the *6d* site with anisotropic ADPs. Model 1-X has random disorder of the host structure, where Ga occupies 34.78% and Ge 65.22% of all sites. Overall, three different constraints were used; (1) a chemical constraint where the total sum of Ga and Ge atoms in the unit cell is 16 and 30, respectively (chemical), (2) an occupancy constraint fixing all host sites to be fully occupied (occupancy), and (3) a thermal vibration constraint, where the ADPs of the three sites are fixed to be equal (ADP). Different combinations of the three constraints lead to the following models: (2-X) Chemical + ADP, (3-X) Chemical + occupancy, (4-X) Chemical + ADP + occupancy, (5-X) ADP + occupancy, (6-X) Occupancy, (7-X) ADPs fixed to the average value of models 3-X and 5-X. In a final model, 8-X, the ADPs were fixed to the refined neutron ADPs. The rationale behind this is that neutron ADPs generally are considered to be more accurate than those obtained from X-ray diffraction, although socalled X−N refinements may be compromised by differences in systematic errors between the two methods.[26] Detailed results of the resonant X-ray refinements are given

in the Supporting Information. The refined framework occupancies of selected models are also listed in Table 2.

Multitemperature Conventional X-ray Diffraction. Temperature resolved single-crystal X-ray diffraction data were collected with a conventional Bruker APEX II diffractometer using Mo Kα radiation at the Department of Chemistry, University of Aarhus. The single crystal of n-Ba was triangular with dimensions $100 \times 85 \times 50$ μm^3, whereas the p-Ba crystal had dimensions of $85 \times 85 \times 50$ μm^3. Complete data sets were measured at 100, 200, 300, and 400 K with the temperature controlled by an Oxford nitrogen cryostream device. The data were integrated with program SAINT, whereas absorption correction and averaging were carried out using SADABS. The subsequent refinements were carried out with SHELX.[25] Like for the neutron data, the 100 K X-ray data were refined using different models for the position of Ba(2). The same four models were refined with Ba(2) at the *24j* site having isotropic (X-JI) or anisotropic (X-JA) ADPs and with Ba(2) at the *24k* site with isotropic (X-KI) or anisotropic (X-KA) ADPs. The refinements only have minor differences in the reliability factors. Two models, X-I and X-II, were chosen for refining the multitemperature data. In both of these refinements the framework occupancies were fixed to the results of model 4-X from refinement of the resonant synchrotron X-ray diffraction data. In X-I the Ba(2) atom is placed at the *6d* position with anisotropic ADPs, whereas for X-II the Ba(2) is placed at *24j* with an isotropic ADP. The X-I and X-II models have the same number of parameters. Detailed results of the multitemperature conventional X-ray refinements are given in the Supporting Information.

Results and Discussion

Ba(2) Description. The most important issue of the present study is to establish the structural model for Ba(2) in p-Ba and n-Ba. As explained in the introduction, many theories to explain the low κ_L of clathrates implicitly assume that the Ba(2) siting and dynamics must be significantly different in p-Ba and n-Ba. Since the neutron data have no interfering effects of the electron density distribution, they are preferred for establishing the nuclear positions. In Figure 2 we show nuclear difference density contour plots and nuclear difference density isosurfaces for p-Ba (left) and n-Ba (right) based on refinements where Ba(2) has been omitted from the model. The 500 and 700 K data have been omitted from Figure 2 since at these elevated temperatures the Ba nuclear density is highly smeared. The low-temperature data (n-Ba 25 K and p-Ba 15 K) clearly reveal off-center maxima in the nuclear density for both n-Ba and p-Ba. In both cases the maxima are found at the diagonal *24j* site, although the nuclear isosurface is best described as a torus having lower nuclear density at the central *6d* site. Thus, below 100 K Ba(2) appears to be off-center in both n-Ba and p-Ba. The low-temperature structural characteristics of Ba(2) in p-Ba and n-Ba indeed are remarkably similar, and the fundamental difference in thermal conductivity therefore *cannot* be explained by a difference in the Ba(2) siting. With increasing temperature the

(22) Evansa, G.; Pettiferb, R. F. *J. Appl. Crystallogr.* **2000**, *34*, 82−86.
(23) RED, O. D. C., Oxford Diffraction Ltd, Abingdon, Oxfordshire, England, 2004.
(24) Blessing, R. H. *J. Appl. Crystallogr.* **1997**, *30*, 421−426.
(25) Sheldrick, G. M. SAINT-Plus, SADABS, and SHELX programs. University of Göttingen: Germany, 2003.
(26) Iversen, B. B.; Larsen, F. K.; Figgis, B. N.; Reynolds, P. A.; Schultz, A. J. *Acta Crystallogr., Sect. B* **1996**, *52*, 923−932.
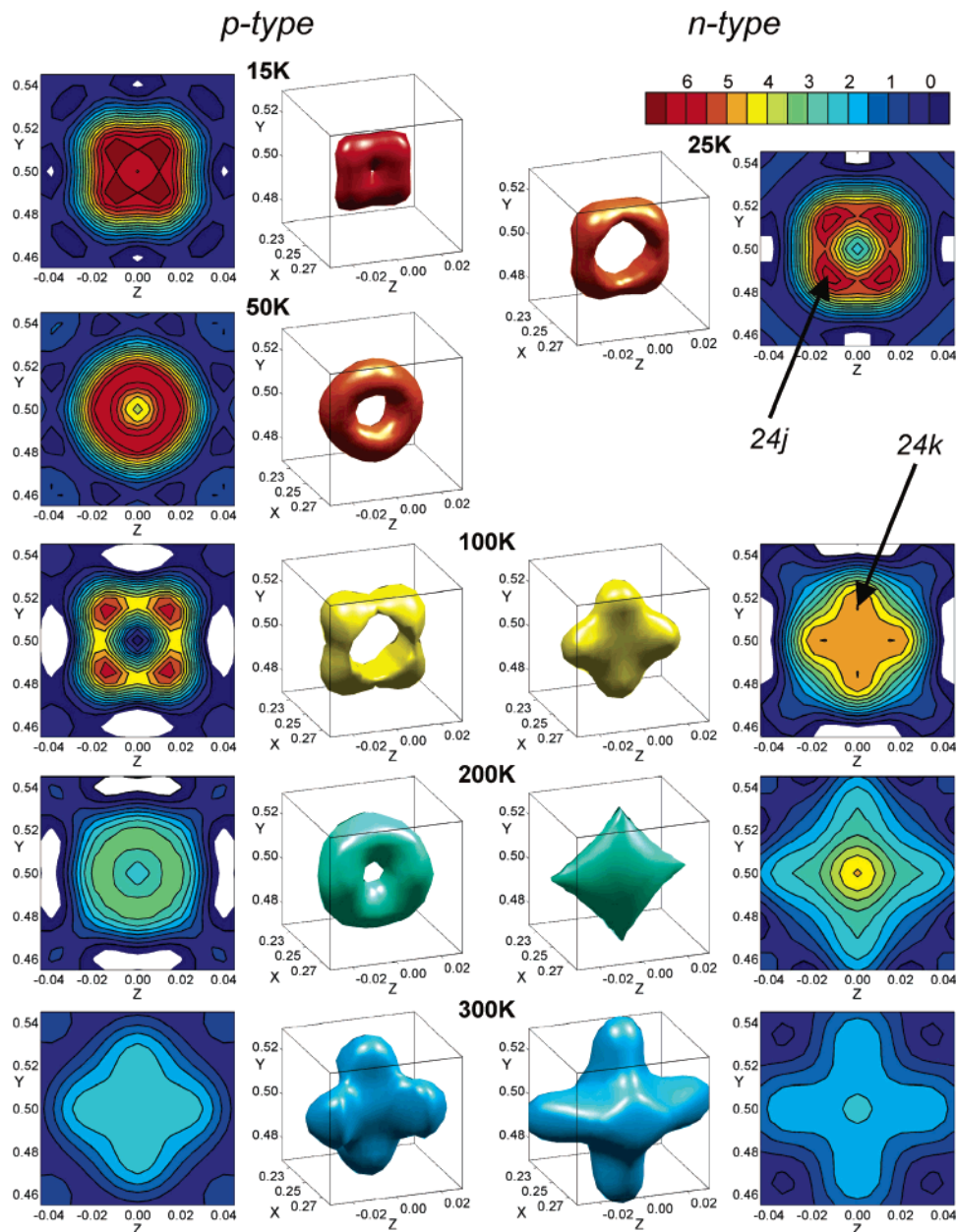
Figure 2. Fourier nuclear difference density maps ($x = 0.25$) and isosurfaces obtained from refining neutron diffraction data with a model omitting Ba2. p-Ba is shown to the left, and n-Ba, to the right.

nuclear density becomes more torus shaped, and at 100 K for n-Ba and 300 K for p-Ba the maxima have shifted to the axial *24k* site. The maxima in nuclear density at the *24k* site of p-Ba were confirmed by the measurement of p-Bas (see Supporting Information). Furthermore, the central *6d* position gets more populated, especially for n-Ba. Thus, with increasing temperature there are subtle differences between p-Ba and n-Ba, which presumably reflect the slightly different potentials felt by the Ba(2) atom due to differences in the Ga/Ge siting. Theoretical calculations for Sr₈Ga₁₆Ge₃₀ predict the opposite behavior for the M(2) guest atoms with the anharmonic vibrational level of lowest energy giving a maximum in the nuclear density at the *24k* position.[27] In the theoretical calculations an increasing temperature leads to the *24j* site being mixed into the Sr(2) nuclear density. For Ba₈Ga₁₆Ge₃₀ the Madsen et al. calculations

predict that Ba is centered on the *6d* site with much reduced anharmonic motion. From the present data it is difficult to determine whether the noncenter maxima observed in the nuclear density for Ba(2) are due to disorder or strong anharmonic motion as in the Sr₈Ga₁₆Ge₃₀ theoretical calculations (or both).[27] However, as pointed out by Bentien et al. the framework disorder of the clathrates means that the real crystal has a different Ga/Ge siting from unit cell to unit cell.[16a] Thus, the cages in the real crystal are not symmetric, but slightly distorted without a well-defined center. This means that the Ba(2) atoms must be slightly displaced from the *6d* site in the individual cages giving an inevitable static disorder component. If there is strong directional bonding between the guest atom and the host structure the noncenter positioning will be enhanced. Since the calculations by Madsen et al. were done on a hypothetical symmetric clathrate structure,[27] they do not

(27) Madsen, G. K. H.; Santi, G. *Phys. Rev. B* **2005**, *72*, 220301.
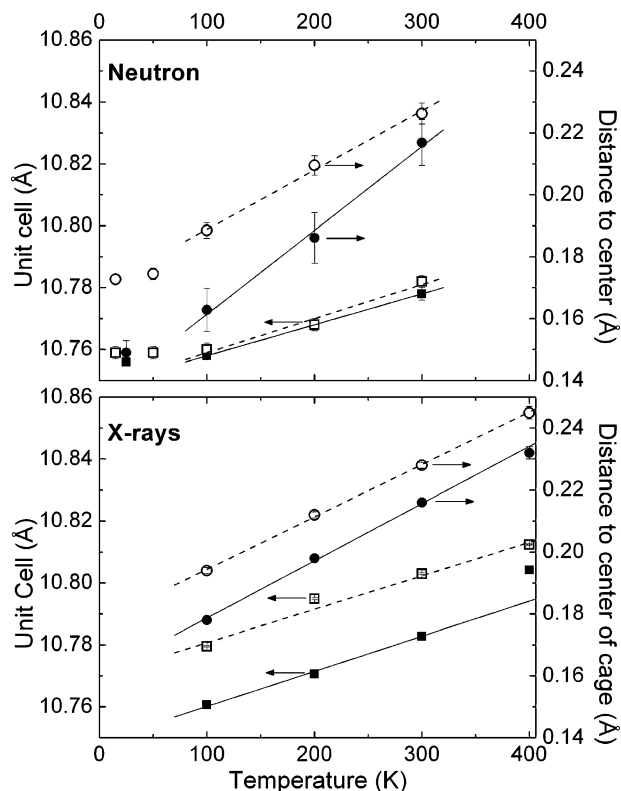
Figure 3. Unit cell parameter and displacement of Ba(2) atom from the cage center (*6d* site) for n-Ba and p-Ba. Filled markers and solid lines refer to n-Ba, whereas open markers and dashed lines are p-Ba.

account for the static disorder. The effect of the asymmetric cage and the specific Ga/Ge siting on the vibrational levels in real clathrates is therefore not known, but it could be the origin of the discrepancy between the low-temperature experimental nuclear density and the theoretical calculations. With regard to κ_L the most important conclusion is that p-Ba and n-Ba both have slightly noncentered Ba(2) atoms and that their low-temperature structural features are very similar. Refinements of the 100 K neutron data using four different models with Ba(2) off-center were inconclusive with regard to the siting because the reliability factors did not distinguish the different models, Table 1. Since no significant improvements were obtained by introducing additional parameters, the model having Ba(2) at the *24j* site with isotropic displacement parameters (3-N) is preferred. This model has the same number of parameters as the 2-N model with Ba(2) in the cage center. The main difference between the two models is that the Ba(2) ADPs decrease dramatically from 2-N to 3-N. The neutron diffraction refinement of $Sr_8Ga_{16}Ge_{30}$ by Chakumakos et al. also had comparable reliability factors for centered and off-centered models even though the Sr(2) is positioned further away from the cage center.[14a]

The refinement of the neutron data as a function of temperature with the 3-N model gives an estimate of the displacement of the Ba(2) atom away from the cage center as a function of temperature. This is shown in Figure 3 together with the cell parameter. Apparently Ba(2) moves linearly away from the center of the cage as a function of temperature. Above 100 K linear fits give slopes of $270(50) \times 10^{-6}$ Å/K and $191(21) \times 10^{-6}$ Å/K for n-Ba and p-Ba, respectively. Linear fits to the cell expansion above 100 K give $100(11) \times 10^{-6}$ Å/K for n-Ba

and p-Ba is $110(14) \times 10^{-6}$ Å/K. Thus, the unit cell expansion is very similar for p-Ba and n-Ba and only about half of the size of the increase in the displacement of Ba(2) from the cage center. Thus, it appears that Ba(2) is moving closer to the host structure atoms with increasing temperature. This is likely due to the Ba(2) atom moving up in an asymmetric potential.

In the refinement of the 100 K single-crystal X-ray diffraction data it is observed that the reliability factors improve as the number of model parameters increase (see Supporting Information). Unfortunately, there is a fairly strong correlation between the refined parameters. For X-JI the correlation between y(Ba(2)) and U_{11}(Ba(2)) is 75% for n-Ba and 71% for p-Ba, whereas the X-KA model for n-Ba has a 98% correlation between x(Ba(2)) and U_{11}(Ba(2)), 87% correlation between z(Ba(2)) and U_{22}(Ba(2)), and 76% between z(Ba(2)) and U_{33}(Ba(2)). Similar correlations are observed for p-Ba with the X-KA model. The large correlations are reflected in the uncertainties on the atomic positions and the ADPs. The X-JI model with Ba(2) on *24j* having isotropic thermal motion was chosen for refining the multitemperature conventional X-ray diffraction data sets. In Figure 3 the displacement of Ba(2) from the *6d* to the *24j* position is shown as a function of temperature. Linear fits give $185(6) \times 10^{-6}$ Å/K and $169(6) \times 10^{-6}$ Å/K for n-Ba and p-Ba, respectively, whereas linear fits to the unit cell expansion give $113(1) \times 10^{-6}$ Å/K and $108(1) \times 10^{-6}$ Å/K. As for the neutron data there is evidence that the Ba(2) atom moves closer to the cage wall with increasing temperature.

The excellent agreement between the neutron and X-ray data gives confidence in the modeling of the off-center Ba(2) atom. Comparison of all the refined distances using equivalent models reveal that Ba(2) is displaced further away from the cage center in p-Ba than in n-Ba. At 100 K the displacements are 0.163(7) Å and 0.188(2) Å for n-Ba and p-Ba, respectively, when determined from the neutron data (0.178(1) and 0.194(1) Å from the X-ray data). The difference in the off-center position between p-Ba and n-Ba is 0.025(7) Å in the neutron case and 0.016(1) Å in the X-ray case. For comparison the Ba^{2+} ion has a radius of about 1.34 Å. In the $Eu_8Ga_{16}Ge_{30}$ and $Sr_8Ga_{16}Ge_{30}$ structures Chakoumakos et al. found M(2) off-center positions of 0.439(3) Å and 0.366(3) Å at 15 K. The M(2) positions were found to be independent of temperature in contrast to the present findings for Ba(2). EXAFS measurements on $Eu_8Ga_{16}Ge_{30}$ and Sr_8Ga_{16}-Ge_{30} give temperature independent off-center distances of 0.45(2) Å and 0.40(5) Å for Eu(2) and Sr(2), respectively.[28] The differences in off-center displacements correspond fairly well to differences in ionic radii Eu^{2+} 1.09 Å (+0.03 Å) → Sr^{2+} 1.12 Å (+0.22 Å) → and Ba^{2+} 1.34 Å. The present data, which have unusually high resolution, suggest a slight difference in the position of Ba(2) in n-Ba and p-Ba, but the difference is only about 1.5% of the ionic radius of Ba^{2+}. It seems unlikely that this minute difference would alter the potential of either a tunnel state model or a soft potential model significantly. In other words this slight difference is hardly significant enough to be the origin of the much discussed dip in the thermal conductivity of *p*-type $Ba_8Ga_{16}Ge_{30}$.

Framework Ordering. The Ga/Ge disorder and vacancies in the host structure will contribute to lowering κ_L, and since 46 out of the 54 atoms belong to the framework, the contribution

(28) Baumbach, R.; Bridges, F.; Downward, L.; Cao, D.; Chesler, P.; Sales, B. *Phys. Rev. B* **2005**, *71*, 024202−02421.9.

may be significant even though the mass difference between Ga and Ge is small. It is therefore crucial to establish the exact framework siting in both n-Ba and p-Ba. Two models were used to refine the framework occupancies against the neutron data. In model 2-N the occupancy was refined with Ba(2) in the center of the cage, and in model 3-N Ba(2) was at the *24j* position with an isotropic ADP. In both cases chemical and occupancy constraints were used. The refined occupancies agree within the uncertainties between the two models, and this shows that the framework occupancies are not affected by the specific modeling of the Ba(2) position. In Table 2 the averages of the occupancies determined from data sets measured below 300 K are listed. For both n-Ba and p-Ba it is observed that Ga prefers the *6c* site and avoids the *16i* and *24k* sites in agreement with previously reported results.[15] Table 2 also includes the refined occupancies from the resonant scattering experiments for the most constrained model (4-X) as well as for the model with freely refined occupancies together with fixed ADPs (7-X). The detailed results from the eight different models are given in the Supporting Information. In general the reliability factors are virtually identical for the different models, and they cannot be used to distinguish between models. This is due to the correlation between the ADPs and the site occupancies. However, the ADPs do give hints about the structural details. In the fully disordered X-ray model (1-X) the ADPs are three times larger than those in the corresponding neutron model. Even so the refined occupancies agree well when the ADPs are fixed to be equivalent (compare models 2-X, 3-X, and 4-X or models 5-X and 6-X). This implies that the refined occupancies are less affected by the constraints than the ADPs. The correlation between the occupancies and the ADPs suggests that it is difficult to obtain quantitative values for the framework occupancies. Model 7-X and 8-X attempt to get around the problem by fixing the ADPs at "reasonable values". In any case the overall trend is very clear. Ga occupies mainly the *6c* site and avoids the *16i* site, whereas the *24k* site contains about half of the total amount of Ga. Model 7-X reveals that all sites have full occupancy within the uncertainties. Defects in the host structure could undermine attempts to extract quantitative site occupancies. The refined compositions from model 7-X are Ba$_8$Ga$_{15.6(1.2)}$Ge$_{29.1(0.7)}$ for n-Ba and Ba$_8$Ga$_{16.1(1.5)}$Ge$_{28.7(9)}$ for p-Ba. This is in agreement with the macroscopic physical property measurements, but it should be noted that the uncertainties are large and one can merely state that the compositions are identical within the uncertainty.

When comparing the occupancies obtained from the resonant X-ray models 4-X and 7-X with the occupancies obtained from the neutron refinements there is agreement within the uncertainties except for the *16i* and *24k* sites in p-Ba. For the smaller n-Ba crystal there is agreement within uncertainties on all sites. Presumably this is due to the refinement of occupancies being slightly affected by the larger extinction correction in the large p-Ba crystal. Overall, the resonance X-ray data are preferred to the neutron data for refinement of occupancies due to the larger scattering contrast. All models agree that *6c* is rich in Ga and that n-Ba contains more Ga than p-Ba at this site. It could be that n-Ba has vacancies at *6c* which will be artificially modeled by an increase in Ga content (Ga is a weaker scatterer than Ge). For highly Ge rich samples vacancies have been observed at the *6c* site.[12b,c] However, the model with free refinement of
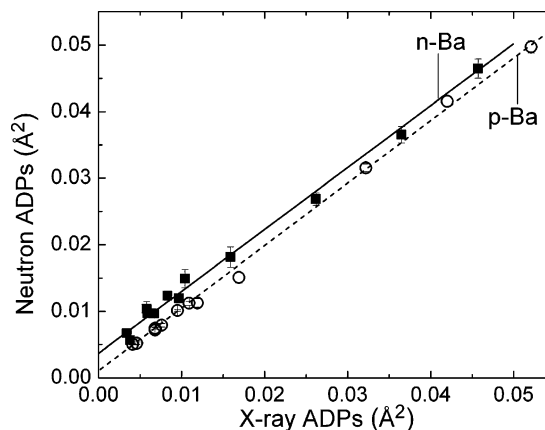

Figure 4. Comparison of ADP values obtained separately from the multitemperature X-ray and neutron data for n-Ba and p-Ba. Filled markers and the solid line refer to n-Ba, whereas open markers and the dashed line is p-Ba.

occupancies (7-X) gives 96(7)% and 98(8)% occupancy on the framework sites for n-Ba and p-Ba, respectively. Therefore the difference in Ga occupancy at the *6c* site between n-Ba and p-Ba appears to be genuine. Even though all our data have been collected with area detectors, we have not been able to detect neither superstructure reflections nor diffuse scattering due to vacancies or disorder. The difference in Ga/Ge occupancy is further corroborated by the small, but significant, difference observed in the unit cell parameters of n-Ba (10.7828(1) at 300 K) and p-Ba (10.8030(3) at 300 K), Figure 3b. It is noteworthy that Ba(2) at the *24k* site is displaced toward the *6c*−*24k* bond of the framework, whereas the *24j* site is closer to the *16i*−*16i* bond of the framework. The above analysis shows that n-Ba has higher Ga content at the *6c* site than p-Ba and that p-Ba has higher Ga content at the *16i* site than n-Ba. The nuclear densities shown in Figure 2 suggest that Ba(2) in n-Ba is at the *24k* position (100 K), whereas Ba(2) is at the *24j* position in p-Ba (100 K). This agrees with a chemical picture where Ba donates valence electrons to the electron depleted Ga−Ga bonds, although one should be cautious against overinterpreting very subtle details.

ADP Modeling. The refined ADPs play an important role in this study since they in principle are fundamental physical properties determined by the lattice dynamics of the crystals. Since the reliability factors are quite similar between the different models, the ADPs can be used to assess the physical correctness of the refined models. In X-ray charge density analysis large efforts are invested to ensure accurate ADP values since correct deconvolution of the thermal motion is essential to the derived results.[29] High symmetry inorganic crystal structures containing heavy elements present a challenging case due to potential absorption, extinction, and anomalous scattering effects. In the present case we have used very small crystals for the X-ray data collections, and in Figure 4 we compare the ADP values obtained separately from the X-ray and neutron data. The agreement is good, which indicates that the data have limited systematic errors.

(29) (a) Coppens, P. *X-ray Charge Densities and Chemical Bonding*; Oxford Science Publications, Oxford, 1997. (b) Iversen, B. B.; Larsen, F. K.; Figgis, B. N.; Reynolds, P. A. *J. Chem. Soc., Dalton Trans.* **1997**, *13*, 2227−2240. (c) Macchi, P.; Larsen, F. K.; Schultz, A.; Iversen, B. B. *J. Phys. Chem. A* **2001**, *105*, 9231−9242. (d) Figgis, B. N.; Iversen, B. B.; Larsen, F. K; Reynolds, P. A. *Acta Crystallogr., Sect. B* **1993**, *49*, 794−806.
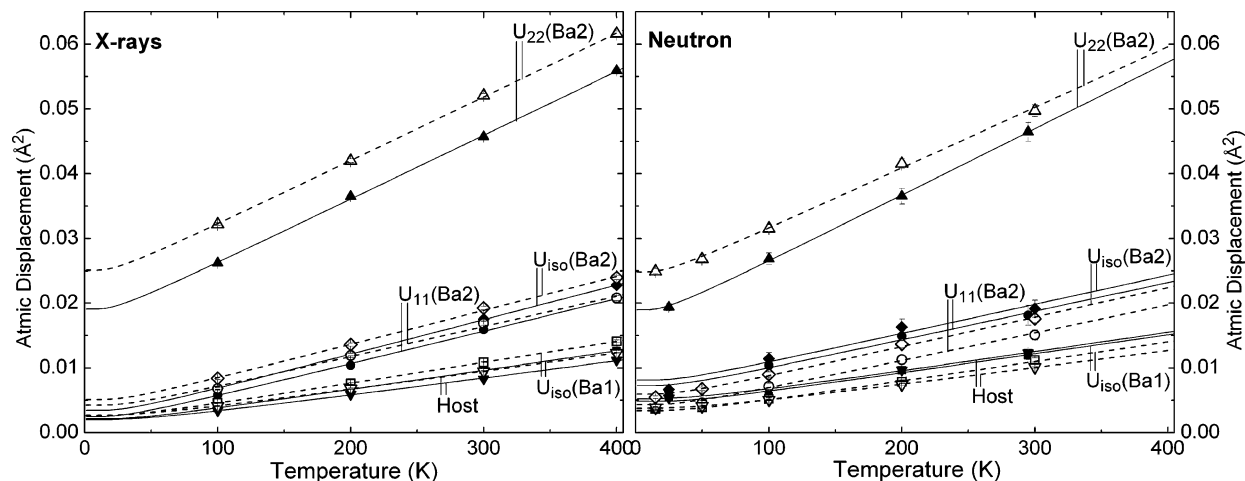
Figure 5. ADPs as a function of temperature for n-Ba (filled) and p-Ba (open) obtained from single-crystal X-ray and neutron diffraction. The lines correspond to fits of the ADPs to a Debye model for the host atoms and an Einstein model for the Ba atoms. n-Ba is shown with filled markers and solid lines, and p-Ba, with open markers and dashed lines.

Table 3. Einstein Temperatures, Debye Temperatures, and Disorder Parameter Obtained from ADP Analysis

	Ba(1) 2a(U_{iso})		Ba(2) 6d(U_{11})		Ba(2) 6d(U_{22})		Debye U_{iso}		Ba(2) 24j(U_{iso})	
	θ_E (K)	d (Å)	θ_E (K)	d (Å)	θ_E (K)	d (Å)	θ_E (K)	d (Å)	θ_E (K)	d (Å)
p-Ba neutron	108(1)	0.043(2)	90(2)	0.046(4)	62(1)	0.148(2)	276(2)	0.044(1)	88(2)	0.063(3)
p-Ba X-rays	104(1)	0.032(1)	87(2)	0.047(7)	60(1)	0.149(1)	267(1)	0.027(1)	82(1)	0.054(4)
n-Ba neutron	109(1)	0.056(6)	89(4)	0.073(6)	59(1)	0.126(1)	259(2)	0.057(1)	88(6)	0.078(9)
n-Ba X-rays	108(1)	0.023(3)	84(1)	0.021(9)	60(1)	0.127(2)	274(3)	0.012(7)	81(1)	0.035(1)
n-Ba Bentien [15a]	124	0.059	101	0.081	73	0.157	416	0.045		
n-Ba Sales [4b]	105	0.046			64[a]	0.117[a]	308	0.052		
n-Ba Blake [32]	129		79		55	0.42(4)				

[a] Based on the isotropic displacement factor.

The framework thermal parameters can be modeled with the Debye expression

$$U_{iso}(T) = \frac{3\hbar^2 T}{mk_B \theta_D^2}\left[\frac{T}{\theta_D}\int_0^{\theta_D/T}\frac{x}{\exp(x)-1}\,dx + \frac{\theta_D}{4T}\right] + d^2$$

where m is the average mass of the Ga and Ge, θ_D is the Debye temperature, and d^2 describes temperature-independent disorder.[16a] The ADPs of the Ba guest atoms can be modeled with an Einstein expression,

$$U_{xx}(T) = \frac{\hbar^2}{2mk_B \theta_{E,xx}}\coth\left(\frac{\theta_{E,xx}}{2T}\right) + d^2$$

where m is the mass of Ba, $\theta_{E,xx}$ is the Einstein energy along the xx direction, and d^2 is a temperature-independent disorder term. The ADPs from neutron model 2-N have been fitted using the Debye and Einstein expression and the results are shown in Figure 5, whereas the fitting parameters are listed in Table 3 together with various literature values for the same parameters. The neutron data measured at 500 and 700 K were not included in the ADP fitting because at these temperatures anharmonic motion becomes very significant.[16a] Thus, modeling of the ADPs would require additional parameters, and direct comparison with the X-ray data would be difficult. The isotropic ADPs of Ba(2) from the 3-N model also have been fitted with the Einstein model, and θ_E values are almost identical for n-Ba and p-Ba. For the models with anisotropic ADPs the lowest Einstein temperature is found for Ba(2) U_{22} at 59(1) K and 62(1) K for n-Ba and p-Ba, respectively. This corresponds to rattler energies

of 5.1(1) meV and 5.3(1) meV in fair agreement with results obtained from phonon density of states measurements by inelastic neutron scattering.[30] The nonzero values of the disorder parameter (d) reflects the off-center siting. Generally, d is higher in n-Ba than in p-Ba except for the Ba(2) U_{22} direction, where it is 0.126(1) Å and 0.148(2) Å for n-Ba and p-Ba, respectively (model 2-N). These values are slightly smaller than the values obtained by direct refinement of Ba(2) at the 24j site. However, the difference in the disorder parameter is 0.022(2) Å between n-Ba and p-Ba in excellent agreement with the difference found for the 24j site refinements (0.025(7) Å). The model with Ba(2) at the 24j site (isotropic ADP) describes the disorder quite well. Thus, d is significantly smaller in the Einstein fits of the ADPs of the 24j model relative to the 6d model. In fact d becomes comparable to the value obtained for Ba(1) in the small cage.

Detailed refinement results obtained from multitemperature conventional X-ray diffraction data are given in the Supporting Information. The derived X-ray Einstein and Debye temperatures are listed in Table 3, and there is good agreement between n-Ba and p-Ba. The fitted disorder parameter, d, is again higher for Ba(2) U_{22} relative to the structural model having Ba(2) at the 24j position with isotropic ADPs. As for the neutron data p-Ba has a larger d value than n-Ba, and the difference is again 0.022(2) Å between the two structures. The agreement between the neutron and the X-ray data indeed is remarkable, and the fact that four different measurements agree so well gives confidence in the estimated Einstein and Debye temperatures.

(30) (a) Hermann, R. P.; Schweika, W.; Leupold, O.; Ruffer, R.; Nolas, G. S.; Grandjean, F.; Long, G. J. *Phys. Rev. B* **2005**, *72*, 174301. (b) Christensen, M.; Juranyi, F.; Iversen, B. B. *Physica B* **2006**, in press.

Additionally, it is noteworthy that the disorder parameter of Ba(2) U_{22} shows the consistent trend that p-Ba is slightly more disordered than n-Ba. Table 3 also includes values obtained from powder diffraction,[16] and these data appear to give larger Einstein and Debye temperatures. The single-crystal neutron experiment by Sales et al.[4b] agrees well with the present work. The theoretical work by Blake et al.[31] highly overestimates the guest atom displacement from the center of the cage. The almost identical values for the Einstein temperature between the neutron and the X-ray data for both n-Ba and p-Ba underlines that the observed difference in the thermal conductivity between these structures cannot be explained by models assuming differences in the displacement of Ba(2). Modeling of the framework ADPs provides estimates of the Debye temperature. Overall the neutron and X-ray data give similar values for n-Ba and p-Ba, but there are small differences. The neutron data, which do not have interfering effects of the electron density, suggest that n-Ba has a slightly larger θ_D than p-Ba (259(2) K versus 276(2) K). This may reflect the differences in the host structures described above.

Conclusion

We have found that the crystal structures of *n*- and *p*-type Ba$_8$Ga$_{16}$Ge$_{30}$ are very similar. All atoms are at the same crystallographic positions with comparable ADP values. Modeling of the temperature dependence of the Ba(2) ADPs in the large cage gives an Einstein temperature of 60(1) K for both n-Ba and p-Ba. Despite the strong overall resemblance between the guest atom position and dynamics in *n*- and *p*-type Ba$_8$Ga$_{16}$Ge$_{30}$ the following subtle differences were observed: (i) The nuclear density appears to shift from the *24j* site to the *24k* site at temperatures between 25 and 100 K for the n-Ba but between 200 and 300 K for p-Ba. (ii) Refinements of the position of Ba(2) reveal that it is less displaced from the center in n-Ba than in p-Ba. The difference was found by neutron diffraction to be 0.025(7) Å and by X-ray diffraction to be 0.016(1) Å. (iii) Analysis of the refined multitemperature ADP values reveal that Ba(2) in the large cage has a larger disorder parameter in p-Ba than that in n-Ba. In the ADP analysis the

difference in the disorder parameter *d* is found to be 0.022(2) Å by both neutron and X-ray diffraction. The main difference between p-Ba and n-Ba is found in the host structure. Refinement of the framework occupancies reveal that in general Ga prefers the *6c* site and avoids the *16i* site, whereas about half of the total Ga content is at the *24k* site. However, it was found that n-Ba contains more Ga at the *6c* site than p-Ba. The refined occupancies give statistical identical compositions Ba$_8$Ga$_{16.1(1.5)}$Ge$_{28.7(9)}$ and Ba$_8$Ga$_{15.6(1.2)}$Ge$_{29.1(0.7)}$ for p-Ba and n-Ba, respectively, in overall agreement with the macroscopic transport properties. In summary, the present structural investigations reveal only subtle differences between the n-Ba and p-Ba structures. It is unlikely that these subtle differences can explain the observed differences in thermal conductivity. The study therefore contradicts models that implicitly assume large structural differences but supports, e.g., the model of strong phonon charge carrier coupling, which only implies small structural differences between n-Ba and p-Ba. It appears that clathrate studies aiming at optimizing thermoelectric properties probably should direct more attention toward the framework.

Supporting Information Available: Results for refinement of different Ba(2) models against 100 K X-ray diffraction data (n- Ba and p-Ba), results for refinement of different models against the multitemperature neutron diffraction data (n-Ba and p-Ba), results for refinement of different models against the resonant synchrotron X-ray diffraction data (n-Ba and p-Ba), results for refinement of the multitemperature conventional X-ray diffraction data (n-Ba and p-Ba), refinement results and a Fourier difference map for p-Bas. This material is available free of charge via the Internet at http://pubs.acs.org.

JA063695Y

(31) Blake, N. P.; Bryan, D.; Latturner, S.; Møllnitz, L.; Stucky, G. D.; Metiu, H. *J. Chem. Phys.* **2001**, *114*, 10063−10074.